





## ORIGINAL PAPER

# Ratio of stemness to interferon signalling as a biomarker and therapeutic target of myeloproliferative neoplasm progression to acute myeloid leukaemia

Fabiola Attié de Castro<sup>1,2</sup>  | Parinaz Mehdipour<sup>1,3</sup> | Ankur Chakravarthy<sup>1</sup> | Ilias Ettayebi<sup>1,4</sup> | Helen Loo Yau<sup>1,4</sup> | Tiago Silva Medina<sup>1,5</sup> | Sajid A. Marhon<sup>1</sup> | Felipe Campos de Almeida<sup>1,6,7</sup>  | Thiago Mantello Bianco<sup>8</sup> | Andrea G. F. Arruda<sup>1</sup> | Rebecca Devlin<sup>1</sup> | Lorena Lobo de Figueiredo-Pontes<sup>8</sup> | Fernando Chahud<sup>9</sup> | Maira da Costa Cacemiro<sup>2</sup> | Mark D. Minden<sup>1</sup> | Vikas Gupta<sup>1</sup>  | Daniel D. De Carvalho<sup>1,4</sup> 

<sup>1</sup>Princess Margaret Cancer Centre, University Health Network, Toronto, Ontario, Canada

<sup>2</sup>Department of Clinical Analysis, Toxicology and Food Sciences, School of Pharmaceutical Sciences of Ribeirão Preto, University of São Paulo, Ribeirão Preto, Brazil

<sup>3</sup>Nuffield Department of Medicine, Ludwig Institute for Cancer Research, University of Oxford, Oxford, UK

<sup>4</sup>Department of Medical Biophysics, University of Toronto, Toronto, Ontario, Canada

<sup>5</sup>Translational Immuno-Oncology Group, International Research Center, A.C. Camargo Cancer Center, São Paulo, Brazil

<sup>6</sup>Instituto de Ciências Biomédicas, Universidade de São Paulo, São Paulo, Brazil

<sup>7</sup>Instituto de Investigação em Imunologia, Institutos Nacionais de Ciência e Tecnologia (INCT-iii), Salvador, Brazil

<sup>8</sup>Hematology Division, Department of Medical Imaging, Hematology and Clinical Oncology, Ribeirão Preto Medical School, University of São Paulo, Ribeirão Preto, Brazil

<sup>9</sup>Department of Pathology and Forensic Medicine, Ribeirão Preto Medical School, University of São Paulo, Ribeirão Preto, Brazil

## Correspondence

Daniel D. De Carvalho, Princess Margaret Cancer Centre, University Health Network, Toronto, ON, Canada.

Email: [daniel.decarvalho@uhnresearch.ca](mailto:daniel.decarvalho@uhnresearch.ca)

Fabiola Attié de Castro, Department of Clinical Analysis, Toxicology and Food Sciences, School of Pharmaceutical Sciences of Ribeirão Preto, University of São Paulo, Ribeirão Preto, SP, Brazil.

Email: [castrofa@fcfrp.usp.br](mailto:castrofa@fcfrp.usp.br)

## Funding information

Canadian Network for Research and Innovation in Machining Technology, Natural Sciences and Engineering Research Council of Canada, Grant/Award Number: 489073; Elizabeth and Tony Comper MPN Program at Princess Margaret Cancer Centre; Fundação de Amparo à Pesquisa do Estado de São Paulo, Grant/Award Number: 2015/21237-4, 2015/21866-1 and 2017/03019-5; Guglietti Fellowship PMC Foundation; Hold'em for life Post-doctoral fellowship; Institute of Cancer Research, Grant/Award Number: 201512MSH-360794-228629 and 148430; Instituto

## Summary

Progression to aggressive secondary acute myeloid leukaemia (sAML) poses a significant challenge in the management of myeloproliferative neoplasms (MPNs). Since the physiopathology of MPN is closely linked to the activation of interferon (IFN) signalling and that AML initiation and aggressiveness is driven by leukaemia stem cells (LSCs), we investigated these pathways in MPN to sAML progression. We found that high IFN signalling correlated with low LSC signalling in MPN and AML samples, while MPN progression and AML transformation were characterized by decreased IFN signalling and increased LSC signature. A high LSC to IFN expression ratio in MPN patients was associated with adverse clinical prognosis and higher colony forming potential. Moreover, treatment with hypomethylating agents (HMAs) activates the IFN signalling pathway in MPN cells by inducing a viral mimicry response. This response is characterized by double-stranded RNA (dsRNA) formation and MDA5/RIG-I activation. The HMA-induced IFN response leads to a reduction in LSC signature, resulting in decreased stemness. These findings reveal the frequent evasion of viral mimicry during MPN-to-sAML progression, establish the LSC-to-IFN expression ratio as a progression biomarker, and suggests that HMAs treatment can lead to haematological response in murine models by re-activating dsRNA-associated IFN signalling.

Fabiola Attié de Castro and Parinaz Mehdipour contributed equally to this work.

This is an open access article under the terms of the [Creative Commons Attribution-NonCommercial](https://creativecommons.org/licenses/by-nc/4.0/) License, which permits use, distribution and reproduction in any medium, provided the original work is properly cited and is not used for commercial purposes.

© 2023 The Authors. *British Journal of Haematology* published by British Society for Haematology and John Wiley & Sons Ltd.

Nacional de Ciência e Tecnologia da Criosfera;  
 Conselho Nacional de Desenvolvimento  
 Científico e Tecnológico; Ontario Institute for  
 Cancer Research (OICR)

## KEY WORDS

DNA hypomethylating agents, DNA methylation, interferon response, leukaemia stem cells, myeloproliferative neoplasm, secondary acute myeloid leukaemia, viral mimicry

## INTRODUCTION

*BCR-ABL1*-negative myeloproliferative neoplasms (MPNs) are haematopoietic malignancies characterized by a clonal proliferation and apoptosis resistance of progenitor and mature myeloid cells, which is thought to arise from a mutated haematopoietic stem cell (HSC).<sup>1–3</sup> Classical MPNs include essential thrombocythaemia (ET), polycythaemia vera (PV) and primary myelofibrosis (PMF).<sup>4</sup> Among them, PMF has the worst prognosis, characterized by bone marrow (BM) fibrosis and an increased risk of transformation to secondary acute myeloid leukaemia (sAML).<sup>5</sup>

Many of the genetic characteristics of MPNs have been well established and feature a prominent activation of JAK–STAT signalling pathway in MPN pathogenesis.<sup>6</sup> The driven genetic mutations in MPN, the JAK2V617F, CALR and MPL trigger the signal transducers and activators of transcription 1/3/5 (STAT1/3/5) pathways through JAK2 activation. These mutations mainly occur in a mutually exclusive manner among MPN patients, with JAK2V617F being the most common mutation.<sup>6</sup> The JAK2V617F mutation is present in mature and maturing myeloid cells and plays a role in sustaining the stem cells involved in disease development.

The activation of JAK/STAT pathway through JAK1/TYK2- and JAK/STAT-independent signalling pathways (non-canonical pathway) are critical for interferon type I (IFN I) signalling and the expression of interferon-stimulated genes (ISGs).<sup>7</sup> The activation of JAK1/TYK2 phosphorylates and activates STAT1 and STAT2 proteins, leading to transcription of ISGs.<sup>8</sup> This highlights a prominent role of IFN signalling in MPN physiopathology. Furthermore, JAKs phosphorylate and induce the formation of STATs complexes, such as STAT1, which is associated with a pro-inflammatory response.<sup>8</sup>

Targeting the stem cells to prevent disease progression presents a potential therapeutic strategy for MPNs.

In addition to the canonical JAK2/CALR/MPL mutations, MPN patients can also present other somatic mutations such as ASXL1, EZH2, SRSF2, IDH1, IDH2 and TET2. Among those, somatic mutations in ASXL1, EZH2, SRSF2 and IDH1/2 are associated with increased risk of premature death or leukaemic transformation.<sup>9</sup>

However, despite increased understanding of the molecular features associated with MPN initiation and progression, identification of biomarkers associated with progression and therapeutic strategies to prevent or delay the onset of progression remains as an area of unmet medical need.

Here, we describe that the activation of IFN signalling and frequency of leukaemia stem cells (LSCs) is anti-correlated in large cohorts of AML patients. Moreover, MPN progression to sAML is characterized by a decrease in canonical IFN

signalling and an increase in LSC frequency. This increase in the ratio of stemness to IFN signalling has the potential to identify MPN patients at higher risk based on DIPSS scores and genomic profile, and it can select for MPN primary cells with higher colony forming potential. Finally, we also observed that DNA hypomethylating agents (HMAs) are able to induce viral mimicry, characterized by double-stranded RNA (dsRNA) formation, activation of dsRNA sensing machinery and activation of IFN signalling in sAML cell lines. Moreover, HMAs are able to abolish colony forming capacity, induce activation of IFN pathway, decrease expression of LSC genes in primary MPN cells and induce IFN signalling and haematological responses in a murine model of Jak2V617F MPN. Altogether, our results suggest that the ratio of LSC to IFN signatures is a potential biomarker for MPN progression that can be pharmacologically modulated by HMAs in MPN.

## METHODS

### Analysis of publicly available AML datasets

We obtained the IFN and LSC signatures from previous literature.<sup>10,11</sup> AML RNA-seq data were obtained from SAGE Synapse for TCGA AML. Processed RMA normalized data were obtained for the AML dataset GSE6891 and GSE30377<sup>11</sup> from the Gene Expression Omnibus, and for E-MTAB-3444, raw CEL files were downloaded from EBI Array Express and normalized using fRMA<sup>12</sup> normalization. For purposes of analysis, probes were collapsed to genes for each Affymetrix dataset using the most variable probe. Clustering of the correlation matrix and Pearson's correlation on ssGSEA scores were used to evaluate relationships between the IFN and stemness signatures.

### Patients' samples

For the NanoString gene expression assay of LSC and IFN pathway-related genes (Table S2), we used 87 patients (72 MPN at chronic phase [CP]—9 polycythemia vera [PV], 6 ET, 20 PMF, 20 post-ETMF and 17 post-PVMF—and 15 sAML; Table S1A). All patient samples and clinical data were collected after obtaining written informed consent from patients using research and ethics board approved consent (UHN: REB number 16-5055).

The RNA-Seq analysis was performed for 12 MPN–sAML paired samples (progressor group) and 5 MPN CP patient samples collected in two CP time points (non-progressor group) (Table S1B). All the patient samples were obtained from the Princess Margaret malignant haematology tissue

bank. The MPN and sAML patients included in this study were diagnosed according to World Health Organization classification of myeloid neoplasms, 2016.<sup>4</sup>

## Myeloid cells isolation

Peripheral blood mononuclear cells (PBMCs) from MPN and sAML patients were stained with SYTOX™ blue dead cell stain (Thermo Fisher Scientific) and then labelled with human anti-CD3-APC (BD Pharmingen™) and human anti-CD19-PE-Cy7 (BD Pharmingen™) antibodies. Afterwards, viable cells (sytox blue negative) negative for CD3 and CD19 markers were sorted by using FACSARIAIII (BD BioSciences). The sorted fraction was checked for purity by acquiring 5000–10 000 events and used for different assays.

## NanoString gene expression assay

RNA from patients and control's myeloid cells was isolated by Qiagen RNeasy MicroKit (Hilden) according to the manufacturer's protocol. Seventy nanograms of total purified RNA from sorted PBMC (CD3<sup>+</sup>CD19<sup>+</sup>) from 87 patients (Table S1A), sAML cell lines pre- and post-5-AZA-CdR treatment and malignant HSCs (CD34<sup>+</sup>CD38<sup>+</sup>) from 11 PMF/myelofibrosis (MF) patients from Groups 1, 2 and 3, was analysed by NanoString gene expression assay according to manufacturer's protocol (NanoString Technologies).

## In vitro culture of human MF primary cells

PBMCs from MF patients were cultured in StemSpan™ SFEM II (Stem Cell Technology) supplemented with human recombinant (rh) Flt3/Flk-2, rh IL-3, rh GM-CSF, rh IL-6, human stem cell factor and rh G-CSF (Stem Cell Technology).

## dsRNA enrichment assay

Around 100 000 viable HEL 92.1.7, SET-2, UKE-1 and MARIMO cells were collected after 4 days of 5-AZA-CdR (Sigma) treatment. Samples were then stained with live/dead fixable aqua (ThermoFischer Scientific) following manufacturer's instructions. The cells were then stained with K1 anti-dsRNA (Scicons)—conjugated to APC (lightning-link APC labeling kit) or Isotype K1 IgG2a-APC conjugated antibodies. Flow cytometry was performed on stained cells to quantify the dsRNA enrichment.

## Colony forming assay

Unsorted MF or sAML patient primary cells or HEL 92.1.7 cell line were treated for three consecutive days with 5-AZA-CdR. The cells were washed out and seeded in drug

free media for 4 days. Then 50 000 viable MF or 15 000 sAML primary patient cells or 5000 HEL 92.1.7 viable cells were plated in triplicate onto MethoCult™ H4534 Classic Without EPO (Stem Cell Technology). After 12–14 days of culture, the colonies were quantified under an inverted microscope.

## CRISPR knock-out

In order to generate HEL 92.1.7 and primary sAML knock-out (KO) samples, CRISPR Cas9 system from IDT was used based on the manufacturer protocol. Briefly, ribonucleoprotein (RNP) complex was assembled by mixing of Alt-R® CRISPR-Cas9 CrRNA (Table S6) with Alt-R CRISPR-Cas9 tracrRNA and Alt-R HiFi S.p. Cas9 Nuclease V3. After assembly of RNP complex and its mixture with Cas9, it was transfected into the target cells by electroporation using pulse code EH115 and Lonza P3 primary cell 4D- Nucleofactor™ X Kit S.

## Mice

We used the conditional Jak2V617F knock-in model<sup>13</sup> in C57BL/6 CD45.2 background and the wild-type C57BL/6 CD45.1 mouse strain, both housed in a sterile barrier facility at the Medical School of Ribeirão Preto, University of São Paulo. All experiments were approved by the Institutional Animal Ethics Committee (Protocol no. 066/2016) and performed according to the IACUC guidelines. The Jak2V617F mice were generated, as previously described,<sup>14</sup> by breeding mice that carry the silent mutation (Jak2 wt/Fl) with mice harbouring Cre-recombinase. Briefly, Cre expression in Jak2 wt/Fl mice results in an inversion of the mutant exon that corrects its transcription direction followed by excision of the wild-type exon. The JAK2V617F mutation has a 100% penetrance and leads to a phenotype that is very similar to the human PV as early as 4 weeks after birth. We used Vav-iCre transgenic mice (C57BL/6 background) to generate Jak2 wt/Fl Cre+ (Jak2V617F) and Jak2 wt/wt Cre+ (Jak2WT) mice. Eight-week old mice (five females and five males) from C57BL/6 B6.SJL-Ptprca Pepcb/Boy (CD45.1) were used as BM transplantation recipients.

## RESULTS

### Inverse correlation between IFN signalling and LSC signature in multiple AML datasets

We initially assembled and analysed a large collection of AML patient transcriptome datasets, from two large publicly available Affymetrix cohorts (GSE6891 [ $n=537$ ] and E-MTAB-3444 [ $n=660$ ]) and TCGA ( $n=174$ , RNAseq) totalling 1371 samples. Using these large datasets, we observed that a LSC gene signature ( $n=49$  genes)<sup>11</sup> and an IFN response gene set known to be induced by HMA ( $n=22$  genes)<sup>10</sup> were anti-correlated (Figure 1A–C). Upon cluster analysis of the samples according to the expression pattern

of these gene sets, we found most samples segregated by LSC and IFN gene set membership (Figure S1A–C). Then, we performed a deconvolution-based analysis of the bulk profiles using the CIBERSORT algorithm<sup>15</sup> and genes differentially expressed between LSC<sup>+</sup> and LSC<sup>−</sup> fractions in GSE30377 cohort.<sup>11</sup> Upon segregating samples into those with high and low LSC<sup>+</sup> fraction cells (Figure S1D–F), we observed significantly higher ssGSEA scores for the IFN signature in LSC-low samples across all three datasets, offering evidence for the existence of a mutually antagonistic relationship between stemness and IFN pathway activation in primary AML at diagnosis (Figure 1D–F).

### The high IFN and low stemness signatures are preserved in MPN preleukaemic conditions and their imbalance is associated with disease progression

Subsequently, in order to probe this association in a collection of MPNs and sAML samples, we used an *in house*

cohort of patient samples ( $n=87$  samples) and a custom NanoString platform to examine the transcriptional patterns of subsets of IFN pathway and stemness genes. We assayed gene expression in peripheral blood sorted myeloid cells (CD3<sup>−</sup>CD19<sup>−</sup>) from 72 MPN patients and 15 post-MPN sAML patients (Table S1A).

For each sample, a metagene score was generated by taking the geometric mean of the expression of all the members of the gene set (IFN and stemness respectively). We then estimated if the two metagene scores were correlated within the MPN and sAML patient samples and found a significant inverse correlation between the scores (Figure 2A, Pearson's  $R = -0.46$ ,  $p < 6e^{-6}$ ). Interestingly, the sAML samples showed a higher LSC to IFN ratio (upper left quadrant) than the MPN samples (Figure 2A). The inverse correlation was also reflected upon clustering of the correlation matrix of the individual genes, which highlighted general separation of the two gene sets (Figure S2A,B), further indicating antagonism between LSC and IFN signatures in a gene-by-gene level.

Then, using consensus PAM cluster analysis for LSC and IFN signatures (Figure S2C), three distinct clusters of

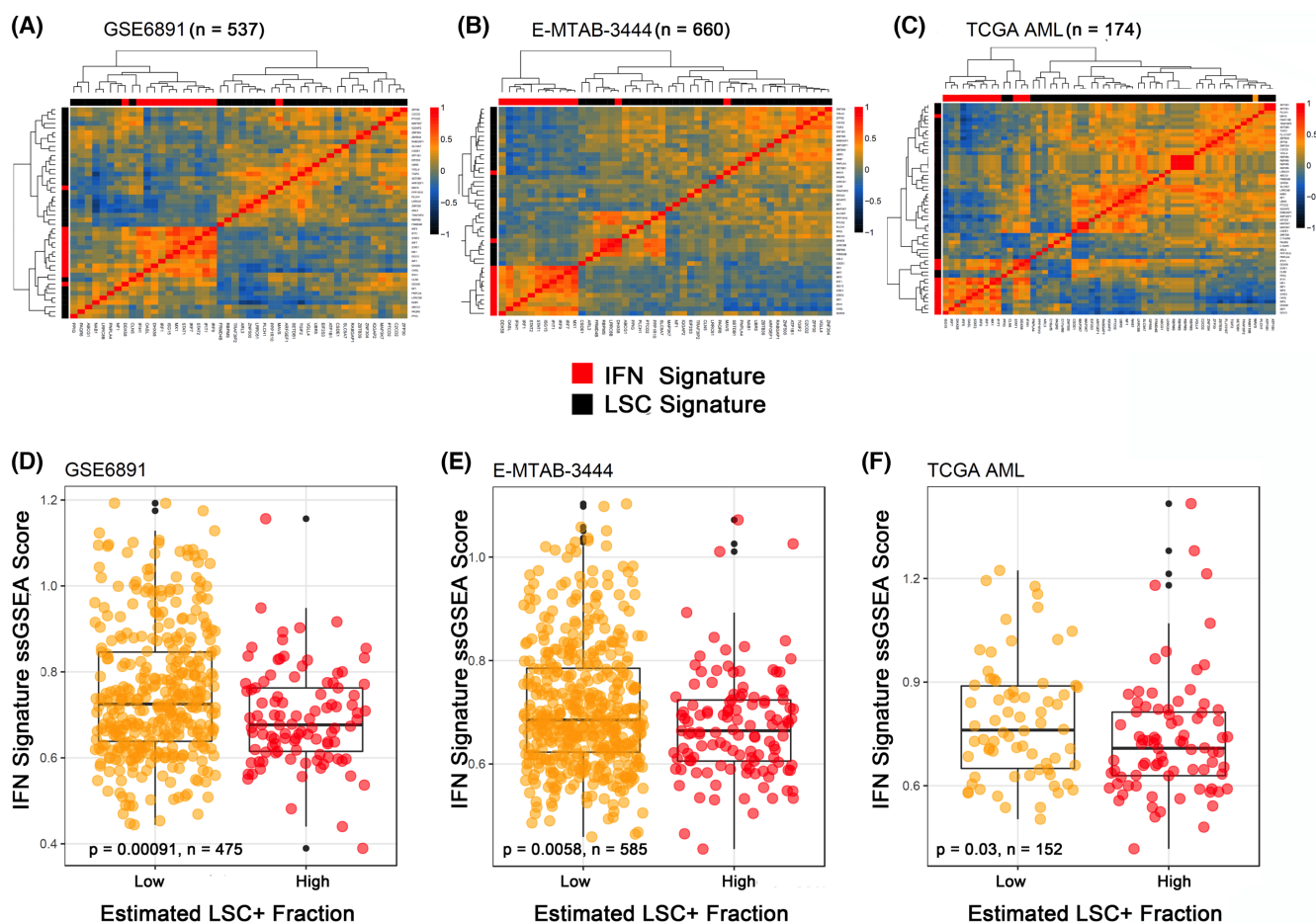


**FIGURE 1** Antagonism of interferon (IFN) signalling and leukaemia stem cell gene expression patterns in acute myeloid leukaemia (AML). (A–C) Heatmaps of correlation matrices between IFN response genes (red) and leukaemia stem cell genes (black) in three large cohorts of primary AML patients. (D–F) ssGSEA scores for IFN signature in samples dichotomized by the estimated fractions of LSC<sup>+</sup> cells by CIBERSORT deconvolution. y Axis = ssGSEA scores for IFN signature, x axis = categories of samples based on LSC<sup>+</sup> cellular fractions,  $p$  values are from Wilcoxon's Rank Sum Test. LSC, leukaemia stem cell.



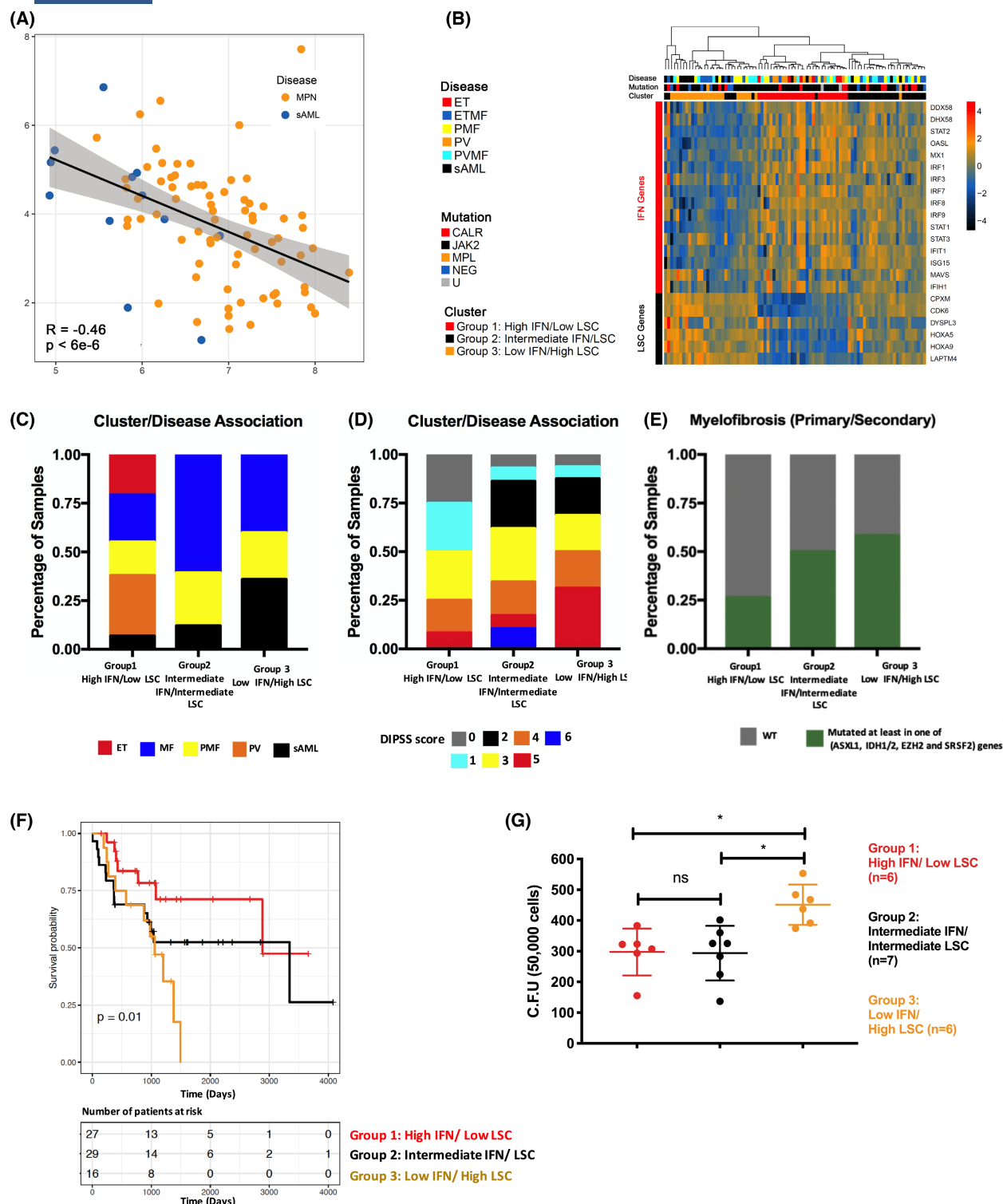


**FIGURE 2** Clustering myeloproliferative neoplasms (MPN)/secondary acute myeloid leukaemia (sAML) patients in three distinct groups based on interferon (IFN) and leukaemia stem cells (LSC) signatures. (A) Correlation scatterplot highlights inverse correlation between IFN and LSC metagene scores. Each dot represents one patient sample. (B) Heatmap showing partitioning of the MPN/sAML dataset into three groups based on IFN and LSC gene set expression. The heatmap is colour-coded based on expression levels (Z-scores). (C) Frequency distribution of each disease per group, showing significant associations between group and disease. (D) Frequency distribution of DIPSS scores for the myelofibrosis patients, showing significant associations at  $p = 0.0007394$ , Fisher's Exact Test. (E) Comparing the frequency of mutation in at least one of the genes associated with increased risk of premature death or leukaemia progression, ASXL1, EZH2, SRSF2 or IDH1/2 in each group. (F) Overall survival analysis of MPN patients from the three clusters. The patients from cluster 1 with High IFN/Low LSC have a higher survival rate ( $p = 0.01$ ) than patients from cluster 3 with Low IFN/High LSC. (G) 50 000 myeloid progenitor cells from myelofibrosis primary patients were plated in methylcellulose medium and colony forming units were scored after 12–14 days for colony-forming ability evaluation. Data are represented as the mean number of colonies  $\pm$  standard deviation. Statistical analysis was performed with Kruskal–Wallis followed by Dunnet's multiple comparison test.  $*p < 0.05$ .

samples were defined among the MPN/sAML samples in the dataset: High IFN/Low LSC gene expression (Group 1); Intermediate IFN/Intermediate LSC (Group 2); and Low IFN/High LSC (Group 3) (Figure 2B). There was no significant association between LSC/IFN signatures and MPN driver mutation status (JAK2, CALR, MPL; Figure S2F). However, the disease category was significantly associated with IFN/LSC clusters (Fisher's exact test,  $p=0.0004998$ ). Notably, ET/PV samples were enriched in the High IFN/Low LSC cluster 1, while sAML samples were enriched in the Low IFN/High LSC cluster 3 (Figure 2C; Figure S2D). Moreover, we also calculated the DIPSS scores for the MF patients (PMF/post-ETMF/post-PVMF) and found that patients with higher risk scores were disproportionately included in the Low IFN/High LSC cluster 3, while patients with low risk scores were enriched in the High IFN/Low LSC cluster 1 (Figure 2D). Furthermore, we observed that patients in the Low IFN/High LSC cluster 3 and intermediate IFN/intermediate LSC cluster 2 had a higher frequency of mutations in genes associated with increased risk of premature death or leukaemia progression, ASXL1, EZH2, SRSF2 or IDH1/2,<sup>9</sup> compared to High IFN/Low LSC cluster 1 patients (Figure 2E; Figure S2E,F). The presence of the TP53 mutation was not analysed in this cohort. Additionally, the overall survival rate assessed in the patients from the three distinct clusters, indicated that patients from High IFN/Low LSC cluster 1 had a higher survival rate than patients from Low IFN/High LSC cluster 3 ( $p=0.01$ ) (Figure 2F).

Finally, we tested whether patient samples from the three IFN/LSC clusters have distinct clonogenicity capacities. We plated a total of 19 PMF/MF patient PBMC samples from the three IFN/LSC clusters in methylcellulose and counted the number of colonies after 12–14 days of incubation. Patient samples from the Low IFN/High LSC cluster 3 showed significantly higher colony formation potential compared to both High IFN/Low LSC cluster 1 and intermediate IFN/intermediate LSC cluster 2 samples (Figure 2G). To determine whether or not the change in IFN/LSC ratio between the three clusters was due to differences in LSC frequency and population dynamics, we assessed the IFN/LSC gene signatures in the CD34<sup>+</sup>CD38<sup>−</sup> sorted fraction (malignant HSC cell population)<sup>16,17</sup> of the same PMF/MF patients used in the gene expression signature evaluation. The CD34<sup>+</sup>CD38<sup>−</sup> frequency did not show any significant difference among the distinct three groups (Figure S2G). Additionally, gene expression analysis from sorted CD34<sup>+</sup>CD38<sup>−</sup> cells presented a similar pattern of IFN/LSC ratio to the PBMC CD3<sup>−</sup>CD19<sup>−</sup> population, indicating that the IFN/LSC ratio detectable in the bulk population can be used for clustering MPN patients into three clusters<sup>6</sup> (Figure S2H).

To validate our findings, we performed RNA-seq on 12 matched pairs of MPNs in chronic and sAML phases (Progressors group) and five MPN patients who had not progressed to sAML, at two different time points of follow-up (Non-Progressors group) (Table S1B; Figure 3A). When summarizing the expression of the IFN pathway and LSC signatures using ssGSEA scores, a significant decrease in IFN

gene expression signature upon the transition to sAML and a significant increase in the LSC gene expression signature were observed (Figure 3B). This was reflected in the continued preservation of the inverse correlation between IFN and LSC gene expression in this cohort (Figure 3C; Pearson's  $R=-0.59$ ,  $p=0.0022$ ). Again, in this paired cohort, the sAML group showed a decrease in IFN and an increase in LSC as they progressed (Figure 3D). The significant decrease in IFN signalling, when patients progressed, was associated with a decrease in transcripts (IR-alsu) that can form dsRNAs<sup>18</sup> (Figure S3A). Finally, we found multiple IFN pathway-related and LSC genes to be differentially expressed upon Restricted Hypothesis Testing of the expression data (fold change > 1.5, false-discovery rate [FDR] < 0.1) (Figure S3B).

Taken together, these findings confirm that an antagonistic relationship exists between IFN signalling and stemness in MPNs, and modulation of this axis characterizes disease progression and aggressiveness. This data highlights a potential use of these signatures for disease stratification. Moreover, these results suggest modulating IFN pathway and stemness as a potential therapeutic strategy to avoid or delay progression.

### Treatment with DNA HMAs leads to viral mimicry, IFN response and anti-tumour effects in secondary AML cell lines

HMA is clinically approved for treatment of myelodysplastic syndrome and AML with unfavourable risk, but not for MPN. Our research group and others have previously shown that HMAs act by inducing re-activation of endogenous retroelements, dsRNA formation and consequent activation of the antiviral pattern recognition pathways (MDA5/MAVS/IRF7), leading to IFN pathway activation, a process named viral mimicry.<sup>8,16</sup> Therefore, we sought to investigate the potential of HMAs to counter the downregulation of IFN signalling associated with MPN progression to leukaemia.

We treated four cell lines developed following transformation to AML from MPN, HEL 92.1.7 (JAK2V617F), UKE-1 (JAK2V617F), SET-2 (JAK2V617F) and MARIMO (CALR) with low doses of the HMA, 5-AZA-CdR for 5 days. UKE-1 cells showed the highest sensitivity to HMA (EC50 of 27.2 nM), while MARIMO cells showed the lowest sensitivity (EC50 of 897 nM) (Figure S4A). All four cell lines showed evidence of viral mimicry induction as characterized by dsRNA formation (Figure 4A; Figure S4B) and IFN pathway activation (Figure 4B; Figure S4C). Consistent with drug sensitivity, UKE-1 cells showed the strongest induction of viral mimicry, while MARIMO cells showed the weakest (Figure 4B; Figure S4C). Moreover, HMA treatment led to an increase in apoptosis in cell lines (Figure S4S).

It is well recognized that RIG-I/MDA5 cascades depend on the adaptor molecule MAVS (mitochondrial antiviral signalling)<sup>19</sup> and it is known that it mediates RIG-I and MDA5 activation and connects them to the downstream activation of type I and III IFNs (Figure S5A). In order to evaluate

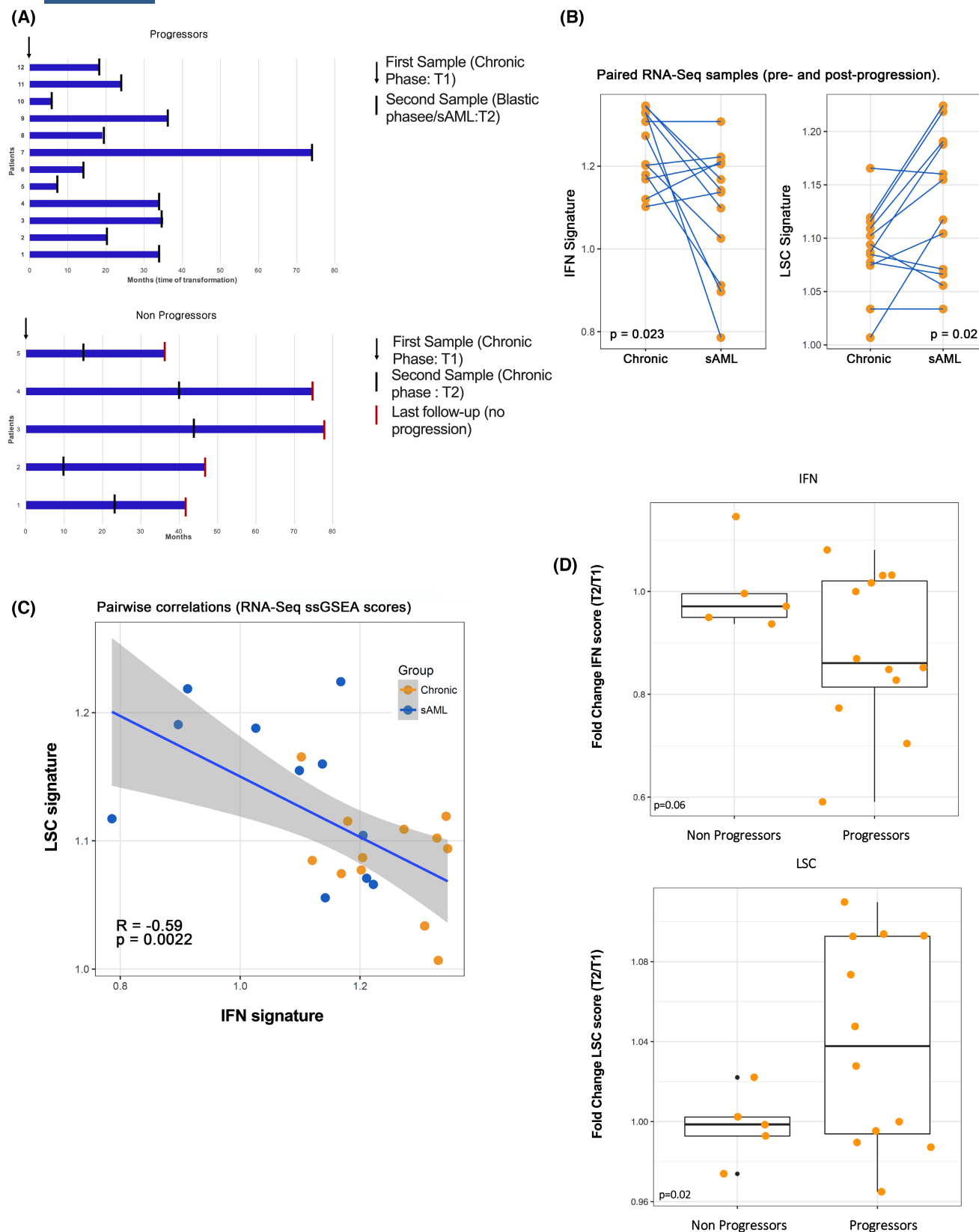


**FIGURE 3** Ratio of leukaemia stem cells (LSC) signature to interferon (IFN) signalling increases during myeloproliferative neoplasms (MPN) to secondary acute myeloid leukaemia (sAML) progression. (A) Timeline for MPN patients' blood sample collection for RNA-seq. (B) Line plots show significant shifts between chronic and sAML for the IFN and LSC signatures in RNA-seq dataset of matched pairs of MPN samples (pre- and post-progression to sAML).  $\gamma$ -Axis shows ssGSEA scores. Statistical analysis was performed with paired  $t$ -test. (C) Correlation scatterplot highlights inverse correlation (Pearson's  $R$ ) between IFN and LSC ssGSEA scores. Each dot represents one patient sample. (D) Boxplots indicate fold changes of IFN (top) and LSC (bottom) ssGSEA scores between paired RNA-seq samples. Statistical analysis was performed with  $t$ -test.

whether the anti-tumour effects of HMA were directly dependent on viral mimicry and its consequent upregulation of IFN signalling, we generated HEL 92.1.7 MAVS-KO cells. MAVS-KO efficiency was evaluated in HEL 92.1.7 by western-blot (Figure 4C) and T7EI mismatch cleavage assay (Figure S5B). We chose HEL 92.1.7 cells because they showed an intermediate response to HMA (Figure S4A) and harbour the most frequent MPN driver gene mutation (JAK2V617F).

We first performed clonogenicity assays following 5-AZA-CdR treatment of HEL 92.1.7 WT (CTRL sgRNA) cells with HEL MAVS-KO cells (MAVS sgRNA) (Figure 4D) and observed a dose-dependent decrease in clonogenicity potential in wild-type HEL 92.1.7 (CTRL sgRNA) cells. Interestingly, this effect was rescued in HEL 92.1.7 MAVS-KO cells (MAVS sgRNA). Similarly, 5-AZA-CdR treatment increased cell death in wildtype HEL 92.1.7 cells and was rescued upon KO of MAVS (Figure S5C). Additionally, we performed gene expression analysis and observed an induction of a subset of ISGs (*IRF7*, *DDX58* and *ISG15*) following 5-AZA-CdR treatment in wild type, but not MAVS-KO cells (Figure 4E).

We next assessed the role of upstream dsRNA pattern recognition receptors following 5-AZA-CdR treatment by generating HEL 92.1.7 RIG-I (known as *DDX58*)-KO (Figure 4F) and MDA5-knockdown (KD) cells (Figure S5D). Both RIGI-KO and MDA5-KD (shMDA5) led to a partial rescue of the effects of 5-AZA-CdR on colony formation (Figure 4G; Figure S5E respectively). Moreover, MDA5 depletion was able to partially rescue the effects of 5-AZA-CdR on cell apoptosis (Figure S5F). We also evaluated the effect of RIGI-KO and MDA5-KD on HMA-induced IFN response (Figure 4H; Figure S5G, respectively) and observed that 5-AZA-CdR induced ISG expression was partially impaired following RIGI-KO and MDA5-KD. These results reinforce the role of dsRNA formation and viral mimicry in HMA-induced IFN response, and suggest that the IFN response partially contributes to the anti-tumour response and decrease in tumour initiation observed following HMA treatment. Interestingly, MAVS, which mediates the signalling of both pathways (MDA5 and RIG-I), plays a major role in mediating the effect of HMA on colony formation and IFN response. Altogether, these results highlight the potential to modulate the IFN signalling in MPN cells using HMA, and suggest the anti-tumour effect of HMA is at least partially dependent on its ability to induce viral mimicry.

### Transient low dose of 5-AZA-CdR decreases colony formation potential of MF primary cells

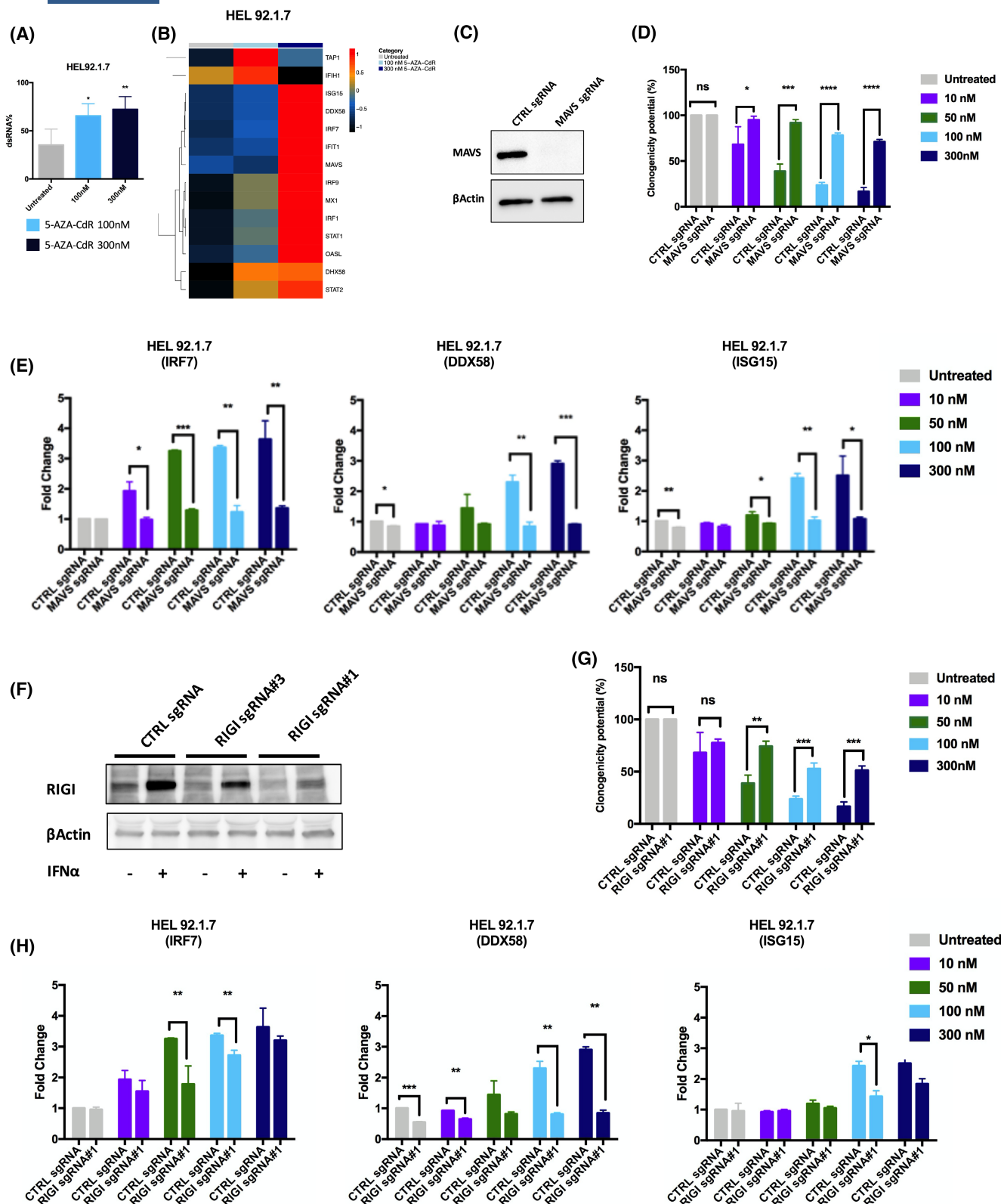
Our results provide evidence that the ratio of LSC to IFN signatures can be modulated by HMAs and this may have a therapeutic benefit. To test this hypothesis further, we evaluated the effects of low-dose HMA treatment in human MF primary cells. We selected 19 PMF/MF patients with

different profiles of LSC and IFN signatures: High IFN/Low LSC ( $n=6$ ), Intermediate IFN/Intermediate LSC ( $n=7$ ) and Low IFN/High LSC ( $n=6$ ) to test whether treatment with transient low dose (10–100 nM) of HMA can decrease colony forming potential. Indeed, we observed marked reduction in colony formation potential in a dose-dependent manner in all the 19 MPN samples from the three clusters (Figure 5A; Figure S5I). Moreover, this reduction in colony formation was associated with increase in four out of eight IFN responsive genes (*DHX58*, *DDX58*, *ISG15* and *STAT1*) and decrease in four out of six LSC genes (*CDK6*, *HOXA5*, *HOXA9* and *DPYSL3*). These genes were evaluated by the NanoString platform performed on PMF/MF untreated and treated with 50 nM of 5-AZA-CdR during three consecutive days (Figure 5B,C). We then knocked-out MAVS in primary sAML samples from Group 1 (High IFN/Low LSC) and Group 3 (Low IFN/High LSC). sAML from Group 3 showed higher clonogenicity potential compared to samples from Group 1 (Figure S5H,J). Consistent with the data from HEL 92.1.7 cell lines, we observed that KO of MAVS in primary sAML samples was able to decrease the effect of 5-AZA-CdR on clonogenicity reduction compared to sAML MAVS-WT cells (CTRL sgRNA) (Figure 5D). Furthermore, MAVS depletion resulted in abrogation of 5-AZA-CdR (50 nM)-induced ISGs expression in sAML samples (Figure 5E).

### Low-dose 5-AZA-CdR in vivo treatment induces ISGs and haematological response in a murine model of Jak2V617F MPN

Next, we used the previously described Jak2V617F knock-in MPN mouse model that resembles human PV<sup>11,12</sup> to test whether in vivo treatment with low-dose HMA leads to haematological response. Given the early lethality when the mutant allele is completely penetrant, we used a transplant model dependent on engraftment of mutant marrow into irradiated recipient mice (Figure 6A). We treated the mice with 0.5 mg/kg 5-AZA-CdR or vehicle for three short cycles (5 days on, 7 days off) followed by two longer cycles (5 days on, 14 days off) (Figure 6A). Chimerism analyses using flow cytometry revealed successful engraftment (Figure S6A–C). Analyses of haematological parameters showed significant decline in red blood cells counts, haemoglobin levels, haematocrit, white blood cells (WBCs) counts and platelet counts up to 24 weeks after initiation of treatment (Figure S6D–H). With the exception of WBCs, all other haematological parameters returned to normal physiological levels and stayed within the normal range even 7 weeks after drug withdrawal (Figure 6D–H). Interestingly, gene expression analysis on PBMC of Jak2V617F knock-in MPN mice treated with 5-AZA-CdR, showed induction of ISGs (Figure 6B), further supporting the role of IFN signalling in durable haematological responses observed following HMAs.





## DISCUSSION

MPNs are preleukaemic disorders characterized by molecular and genetic alterations in HSCs. These HSC abnormalities result in deregulated or ineffective haematopoiesis followed by disease transformation to acute myeloid leukaemia.<sup>20</sup>

MPN leukaemic transformation occurs in treatment-naïve patients and cytotoxic chemotherapy recipients alike, suggesting that disease progression is part of MPN natural history.<sup>1,21</sup> While some clinical parameters are useful for assessing the risk of progression based upon the presence of specific genomic changes, the use of these parameters does

**FIGURE 4** Hypomethylating agent (5-AZA-CdR) effects on secondary acute myeloid leukaemia (sAML) cell lines. (A) Percentage of dsRNA<sup>+</sup> cells measured by fluorescence-activated cell sorting. The results were represented as the mean of the percentage  $\pm$  standard deviation of dsRNA<sup>+</sup> cells. Statistical analysis was performed with Friedman and Dunnett's multiple comparison test. \* $p < 0.05$ , \*\* $p < 0.01$ . (B) Heatmap shows expression level of interferon (IFN) pathway-related genes in HEL 92.1.7 cell line after treatment with the indicated doses of 5-AZA-CdR. The gene expression evaluation was performed in duplicate using NanoString platform and analysed by Nsolver Software. Values were normalized against the *RPLP0* reference gene and referred to untreated control. (C) Western blot analysis of mitochondrial antiviral signalling (MAVS) in HEL 92.1.7 WT (CTRL sgRNA) and MAVS-knockout (KO) (MAVS sgRNA).  $\beta$ -Actin served as the loading control. (D) Clonogenicity potential of HEL 92.1.7 WT and MAVS-KO cells treated with different doses of 5-AZA-CdR. Data are represented as the percentage of colonies counted 12–14 days after seeding 1000 viable cells and  $\pm$  standard deviation. Statistical analysis was performed with unpaired *t*-test. \* $p < 0.05$ , \*\*\* $p < 0.001$  and \*\*\*\* $p < 0.0001$ . (E) Expression profile of a subset of IFN stimulated genes (*ISG15*, *DDX58* and *IRF7*) measured by real-time qRT-PCR in WT (CTRL sgRNA) and MAVS-KO (MAVS sgRNA) HEL 92.1.7 cells. Values were normalized against *RPLP0* reference gene and referred to untreated sample. The results are represented by bars ( $n = 2$ ) and standard deviation of ISG relative expression. Statistical analysis was done by unpaired *t*-test. \* $p < 0.05$ , \*\* $p < 0.01$ , \*\*\* $p < 0.001$ . (F) Western blot analysis of RIGI (*DDX58*) in HEL 92.1.7 WT (CTRL sgRNA) and RIGI-KO (RIGI sgRNA#1 and sgRNA#3) in absence or presence of IFN- $\alpha$  stimulation.  $\beta$ -Actin served as the loading control. (G) Clonogenicity potential of HEL 92.1.7 WT and RIGI-KO (MAVS sgRNA#1) cells treated with different doses of 5-AZA-CdR. Data are represented as percentage of colonies counted 12–14 days after seeding 1000 viable cells and  $\pm$  standard deviation. Statistical analysis was performed with unpaired *t*-test. Statistical analysis was performed by unpaired *t*-test; \*\* $p < 0.01$ , \*\*\* $p < 0.001$ . (H) Expression profile of a subset of IFN responsive genes (*ISG15*, *DDX58* and *IRF7*) measured by real-time qRT-PCR in WT (CTRL sgRNA) and RIGI-KO (RIGI sgRNA#1) HEL 92.1.7 cells. Values were normalized against *RPLP0* reference gene and referred to untreated sample. The results are represented by media bars ( $n = 2$ ) and standard deviation of ISG relative expression. Statistical analysis was done by unpaired *t*-test. Statistical analysis was performed by unpaired *t*-test; \* $p < 0.05$ , \*\* $p < 0.01$ , \*\*\* $p < 0.001$ . dsRNA, double-stranded RNA.

not generalize to MPNs that lack those specific genomic alterations.<sup>9,22,23</sup>

MPN progression to sAML often takes many years to occur, however, once sAML develops, response to intensive treatment is rarely achieved. In this light, the cellular and molecular basis of MPN genesis and progression demand further investigation. Here, we report that distinct patterns of LSC genes and ISGs are associated with disease progression, wherein the least aggressive subtypes/stages show the highest levels of basal IFN signalling and lowest LSC expression, with the relationship being increasingly flipped throughout progression to sAML. This shift is evident not only in samples from different patients representing the spectrum of severity in MPN, but also in matched samples before and after progression. Interestingly, this mutual antagonism also mimics patterns seen in primary AML, suggesting that our work uncovers evidence for a fundamental relationship between an IFN response and stemness in myeloid neoplasms.

JAK-STAT signalling is a key driver of MPN pathogenesis, but IFN signalling is not necessarily the only consequence of JAK-STAT activation in this neoplasia. Indeed, there is a range of inflammatory cytokines<sup>22,23</sup> that are produced by the JAK-STAT pathway distinct from ISG activation. It is well-known that MPN patients present chronic inflammation with enhanced BM and pro-inflammatory circulating cytokines, as well as abnormal activation of leukocytes and platelets, endothelial cell deregulation and increased oxidative stress.<sup>24–26</sup> The elevated levels of pro-inflammatory cytokines play a significant role in driving disease progression, promoting clonal evolution, genetic instability of cells and the proliferation and survival of neoplastic haematopoietic stem cells. Ultimately, this leads to the progression of MPN towards secondary acute myeloid leukaemia.<sup>27–29</sup> The oncoinflammatory response also seems to impair the IFN signalling activation and cell response to IFN- $\alpha$  (IFN $\alpha$ ). The effect of IFN $\alpha$  depends on its interaction with type I IFN receptor (IFNAR1 and IFNAR2c chains), which undergoes

degradation due to pro-inflammatory cytokines stimuli, especially by interleukin-1 and tumour necrosis factor alpha.<sup>30</sup> The low levels of IFNAR1 are associated with an immune evasion mechanism and worse prognosis in solid tumours with an inflammatory microenvironment.<sup>31,32</sup>

The activation of IFN signalling may be a constraint that needs to be progressively disabled to permit the tumour progression including the progression of MPN to MF and sAML. In agreement, in addition to the transcriptional IFN deregulation, defective IFN production as a consequence of immune evasion has also been shown in MPN. For instance, Costa et al. have shown that natural killer cells, known to highly secrete IFN, present an immature profile with deficient cytotoxicity in primary cells from JAK2V617F mice and MF patients.<sup>33</sup>

Indeed, our results agree with recently published data showing that in AML, the expression of repetitive elements is downregulated in LSCs, resulting in the silencing of dsRNA sensing pathways and downstream IFN signalling.<sup>34</sup> This highlights the fundamental importance of suppressing this pathway in the development and persistence of LSCs. Furthermore, our findings identify the ratio of LSC to IFN signalling to be associated with MPN to sAML progression, suggesting these signatures as potential biomarkers for patient stratification.

Consistent with the idea that IFN signalling constrains disease progression, IFN- $\alpha$  treatment in MPN patients has been shown to induce significant clinical responses by multiple indicators.<sup>35,36</sup> IFN $\alpha$  has the ability to reduce myeloproliferation, restore the BM microenvironment, eliminate malignant disease-initiating cells and potentiate the immune response. These effects contribute to achieving haematological remission (normalization of blood counts and resolution of splenomegaly) as well as molecular remission (reduction of allele burden) in MPN patients.<sup>35,36</sup> Moreover, Mosca et al. elegantly reported the direct effect of IFN $\alpha$  against MPN HSCs by promoting their differentiation and exhaustion. They also showed that IFN $\alpha$  treatment is more

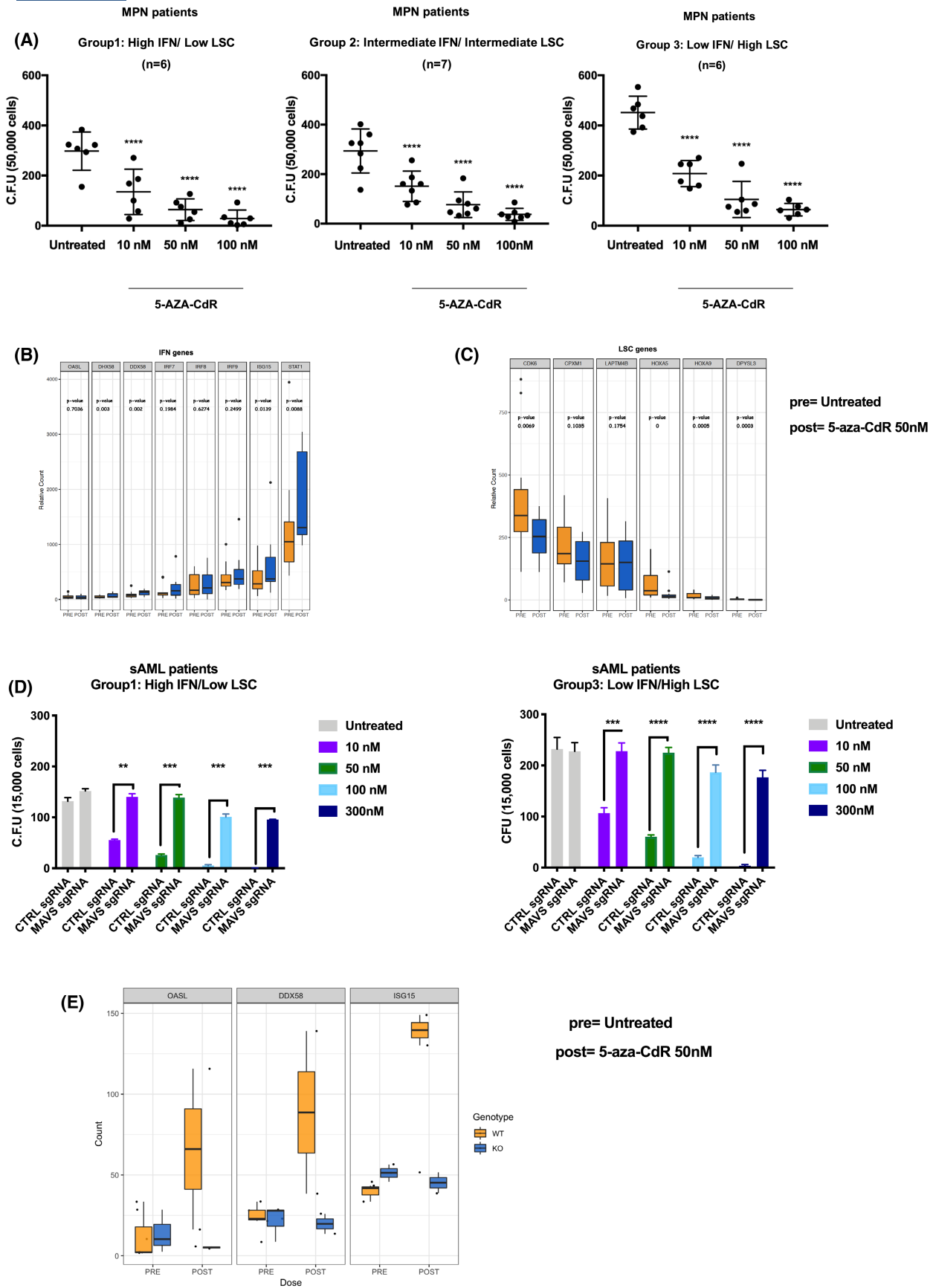


**FIGURE 5** Low dose of AZA-CdR reduces the colony forming ability of myeloproliferative neoplasm (MPN) samples, which is accompanied with induction of interferon (IFN) genes and reduction of leukaemia stem cell (LSC) gene expression. (A) Myeloid progenitor cells clonogenicity results are shown as the number of colonies obtained from colony forming unit assay (CFU assay). Data are represented as mean number of colonies scored 12–14 days after seeding 50 000 viable cells  $\pm$  standard deviation. Statistical analysis was performed with Friedman and Dunnett's multiple comparison test. \*\*\*\* $p < 0.0001$ . (B) Box plots show the gene expression analysis on MPN samples pre- and post-5-AZA-CdR treatment (50 nM) for IFN genes and (C) for LSC genes. To compare the ISG expression and LSC expression level in primary myelofibrosis (PMF) primary cells pre- and post-treatment with 5-AZA-CdR, we applied a binomial generalized linear model to calculate  $p$ -values. (D) Analysis of colony forming ability of WT (CTRL sgRNA) and mitochondrial antiviral signalling-knockout (MAVS-KO) (MAVS sgRNA) secondary acute myeloid leukaemia (sAML) primary samples from Group 1 and Group 3 before and after treatment with different doses of 5-AZA-CdR. Statistical analysis was performed by unpaired  $t$ -test; \*\* $p < 0.01$ , \*\*\* $p < 0.001$  and \*\*\*\* $p < 0.0001$ . (E) Box plots show the gene expression analysis on WT and MAVS-KO sAML primary samples pre- and post-5-AZA-CdR treatment (50 nM) for IFN stimulated genes.

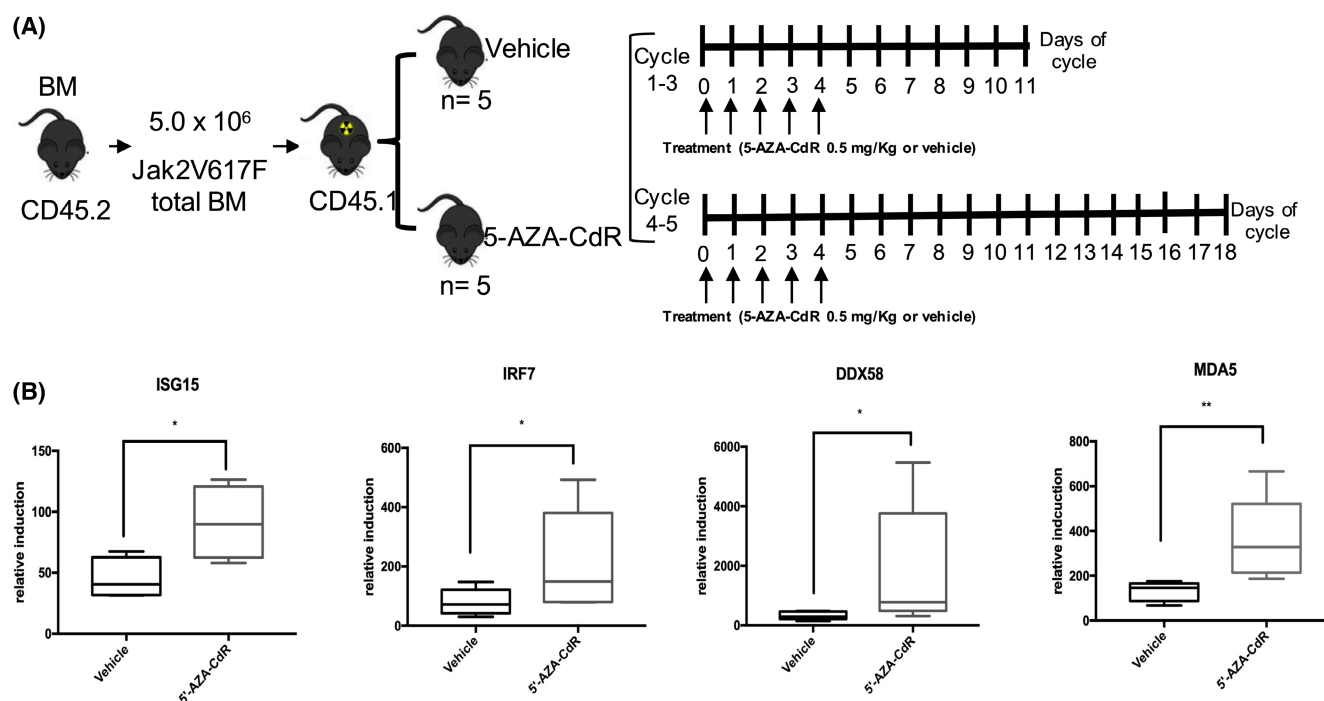


**FIGURE 6** 5-AZA-CdR treatment induces long-term haematological response in a myeloproliferative neoplasm murine model. (A) Experimental strategy of the in vivo treatment of Jak2V617F mice with 5-AZA-CdR. (B) Expression profile of a subset of interferon stimulated genes (*ISG15*, *IRF7*, *DDX58* and *MDA5*) measured by quantitative real-time PCR on mice peripheral blood mononuclear cells at 24 weeks after transplantation. Statistical analysis was performed with Mann–Whitney test. \* $p < 0.05$ , \*\* $p < 0.01$ ; compared to vehicle.

effective in homozygous JAK2V617F<sup>+</sup> HSCs compared to heterozygous JAK2V617F<sup>+</sup> and CALR<sup>+</sup> HSCs.<sup>37</sup>

Our findings support these previous studies showing the direct treatment of IFN in MPN as a strategy to induce remission in CALR mutated patients, to decrease LSC frequency and JAK2 allele burden,<sup>38,39</sup> suggesting a convergence of mechanisms.

Recombinant IFN $\alpha$  is one of the drugs used for cytoreductive therapy in MPN patients at chronic phase (ET, PV and PMF). Despite its clinical effectiveness, IFN $\alpha$  is associated with many adverse effects such as depression, flu-like symptoms, elevated transaminases, fever, nausea, fatigue and vomiting. To decrease these side effects, pegylated IFN has been developed, and has ameliorated the patient acceptability and adherence to treatment.<sup>38,40,41</sup> Pegylated IFN therapy has been associated with a durable haematological and molecular response in JAK2V617F- and CALR-positive patients,<sup>38,39</sup> but the presence of TET2, ASXL1, IDH2 and

TP53 additional mutations is still linked to patient's poorer molecular responses.<sup>38,42</sup> Despite pegylated IFN beneficial effects, it is not yet clear if this therapy will be capable of modifying the MPN natural history and reduce progression to sAML.<sup>40</sup>

Additionally, the use of ruxolitinib, a JAK1/2 tyrosine kinase inhibitor, currently used for treatment of intermediate- and high-risk MF, as well as hydroxycarbamide-resistant PV patients, is not able to impair disease progression or decrease allele burden. Indeed, MPN clonal evolution and transformation to AML has been observed during ruxolitinib monotherapy.<sup>43–45</sup>

The treatment of MPN patients with either the JAK1/2 inhibitor (ruxolitinib) or pegylated-IFN- $\alpha$  may lead to improvement of disease symptoms, a decrease of splenomegaly and a haematological remission. However, only long-term IFN $\alpha$  therapy can eradicate disease-initiating HSCs and reduce disease allelic burden.<sup>46</sup> On the other



hand, the JAK1/2 inhibitor is able to block MPN oncoinflammation, increase the efficacy of IFN $\alpha$  therapy and reduce the risk of cardiovascular events occurring in patients. Thus, there is a mechanistic basis to encourage the use of ruxolitinib combined with pegylated IFN- $\alpha$  (PEGIFN $\alpha$ 2) to treat MPN patients.

The combined treatment of low-dose PEGIFN $\alpha$ 2 and ruxolitinib has demonstrated positive outcomes in the management of PV and MF, such as improvements in blood cell counts, reduction in BM cellularity and fibrosis, decreased JAK2V617F allele burden, relief of symptoms and acceptable levels of toxicity in multiple patients.<sup>47,48</sup> These promising data reinforce the need of combined therapies to achieve the MPN molecular remission and hopefully the cure of the patients.

In our present study, we also identified for the first time that transient and low doses of HMAs can induce IFN signalling by activating a viral mimicry response in MPN cells, characterized by dsRNA formation and MDA5/RIGI and MAVS activation, as described in other cancer types.<sup>10,49</sup> This HMA-induced IFN response in MPN cells leading to a functional decrease in stemness, as measured by colony formation, resulted in long-term improvement of haematological parameters in an MPN mouse model.

Altogether, our results highlight the potential use of HMA for MPN<sup>50,51</sup> as a candidate therapy for early intervention in order to delay the progression of MPNs to sAML without the side effects usually associated with systemic IFN treatment.

The HMAs, such as azacitidine and decitabine, have been used in the treatment of AML, MDS and MDS/MPN. In addition to their direct effects on the AML/MDS/MPN malignant clone, HMAs also induce an immune-mediated anti-tumour response.<sup>52</sup> MPN patients who progress to sAML or SMD are also treated with HMAs, but the response has been disappointing, with a response rate of 38%.<sup>53</sup> In a randomized phase 2 study comparing low-dose decitabine versus low-dose azacitidine in lower risk MDS and MDS/MPN, decitabine therapy showed good tolerability, safety and efficacy. Thirty-two percent of patients treated with decitabine became transfusion independent and 61% presented cytogenetic with a median follow-up of 20 months.<sup>54</sup> Despite the observed efficacy of HMAs in haematological malignancies, higher doses cause cytotoxicity and drug resistance may occur during long-term use.<sup>55</sup>

In MPN murine model, Lock et al.<sup>56</sup> had shown that the combination of 5-Azacitidine and pegylated-IFN $\alpha$  was able to induce disease haematological remission in a JAK2V617F/DNMT3A double-transgenic mice, suggesting that this association may be used for MPN in patients harbouring both mutations.

Considering our findings and the above-mentioned observations from previous studies in MPNs, a potentially curative treatment for MPN and MPN in the accelerated/blastic phase seems to reside in a triple combined therapy, in which JAK2 inhibitor block deleterious oncoinflammation, IFN $\alpha$  and HMA target disease-initiating cells and potentiate anti-tumoural immune response.

In summary, it is plausible that the combination of pegylated IFN $\alpha$ , JAK/STAT inhibitor and a low-dose HMA might be a future treatment modality to be tested in future well-designed clinical studies for patients in the accelerated/transforming phase of MPNs.

## AUTHOR CONTRIBUTIONS

Fabiola Attié de Castro, Parinaz Mehdipour, Ankur Chakravarthy and Daniel D. De Carvalho designed the study, analysed data and wrote the paper. Ankur Chakravarthy, Sajid A. Marhon and Ilias Ettayebi performed all bioinformatics analyses. Fabiola Attié de Castro and Parinaz Mehdipour conducted all in vitro assays. Tiago Silva Medina and Felipe Campos de Almeida conducted the flow cytometry acquiring and analysis. Helen Loo Yau conducted the sAML primary cells knock-out experiments and the flow cytometry acquiring and analysis. Ilias Ettayebi performed also the cell line knock-out and gene expression experiments. Lorena Lobo de Figueiredo-Pontes, Thiago Mantello Bianco, Fernando Chahud and Maira da Costa Cacemiro performed the mice experiments. Vikas Gupta, Mark D. Minden and Andrea G. F. Arruda recruited and selected the patients for the study. Vikas Gupta, Mark D. Minden, Andrea G. F. Arruda and Rebecca Devlin also provided all the clinical data from the myeloproliferative neoplasm and leukaemia patients. Andrea G. F. Arruda was responsible for all regulatory aspects of patient recruitment to the research study.

## ACKNOWLEDGEMENTS

We thank Ann Mullally who kindly donated the JAK2-mutated transgenic mice. We thank PM Genomic Centre for their technical support. We also thank all the members of De Carvalho Lab and the MPN team from Princess Margaret Cancer Centre. Special acknowledgement to Sick Kids flow cytometry core facility for their technical assistance in cell sorting experiments.

## FUNDING INFORMATION

F.A.C. and F.C.A. were recipients of FAPESP (Fundação de Amparo à Pesquisa do Estado de São Paulo, Brazil; BPE 2015/21237-4 and BEPE 2017/03019-5 respectively); P.M. was a recipient of Hold'em for life Postdoctoral fellowship, T.S.M. was a recipient of Conselho Nacional de Desenvolvimento Científico e Tecnológico (CNPq, Brazil). L.L.F.P. is supported by a grant from FAPESP (2015/21866-1). A.C. is supported by a Guglietti Fellowship for Tumour Immunotherapy from the Princess Margaret Cancer Foundation. This work was supported by Grants from Elizabeth and Tony Comper MPN Program at Princess Margaret Cancer Centre (V.G.). D.D.D.C. is supported by the Canadian Institutes of Health Research (CIHR) New Investigator Salary Award (201512MSH-360794-228629), Helen M. Cooke professorship from Princess Margaret Cancer Foundation, Canada Research Chair, CIHR Foundation Grant (FDN 148430), NSERC (489073) and the Ontario Institute for Cancer Research (OICR) with funds from the province of Ontario.

## CONFLICT OF INTEREST STATEMENT

VG received research funding through his institution from Novartis and Incyte pharmaceuticals, and served on the advisory board of Novartis. DDDC received research funding through his institution from Pfizer, and serve in leadership role and own equity in Adela. All the other authors declare no competing financial interest.

## DATA AVAILABILITY STATEMENT

The datasets analysed during the current study are available in the Gene Expression Omnibus repository by the accession number GSE6891 and GSE30377<sup>9</sup> and from the EBI Array Express repository by the accession number E-MTAB-3444. Processed RNA-Seq data have been deposited on Zenodo at <https://doi.org/10.5281/zenodo.1212754>. The RNA-seq raw files could be provided upon request to authors.

## ETHICS STATEMENT

All patient samples and clinical data were collected after obtaining written informed consent from patients using research and ethics board approved consent (UHN: REB number 16-5055). All animal experiments were approved by the Institutional Animal Ethics Committee (Protocol no. 066/2016) and performed according to the IACUC guidelines.

## ORCID

Fabiola Attié de Castro  <https://orcid.org/0000-0003-3347-5873>

Felipe Campos de Almeida  <https://orcid.org/0000-0003-0158-1102>

Vikas Gupta  <https://orcid.org/0000-0002-1419-8607>

Daniel D. De Carvalho  <https://orcid.org/0000-0002-8572-5259>

## REFERENCES

- Campbell PJ, Green AR. The myeloproliferative disorders. *N Engl J Med*. 2006;355:2452–66.
- Tognon R, Gasparotto EPL, Leroy JMG, Oliveira GLV, Neves RP, Carrara RCV, et al. Differential expression of apoptosis-related genes from death receptor pathway in chronic myeloproliferative diseases. *J Clin Pathol*. 2011;64:75–82.
- Tognon R, Gasparotto EPL, Neves RP, Nunes NS, Ferreira AF, Palma PVB, et al. Deregulation of apoptosis-related genes is associated with PRV1 overexpression and JAK2 V617F allele burden in Essential Thrombocythemia and Myelofibrosis. *J Hematol Oncol*. 2012;5:2.
- Arber DA, Orazi A, Hasserjian R, Thiele J, Borowitz MJ, le Beau MM, et al. The 2016 revision to the World Health Organization classification of myeloid neoplasms and acute leukemia. *Blood*. 2016;127:2391–405.
- Barbui T, Barosi G, Birgegard G, Cervantes F, Finazzi G, Griesshammer M, et al. Philadelphia-negative classical myeloproliferative neoplasms: critical concepts and management recommendations from European LeukemiaNet. *J Clin Oncol*. 2011;29:761–70.
- Mead AJ, Mullally A. Myeloproliferative neoplasm stem cells. *Blood*. 2017;129:1607–16.
- Mazewski C, Perez RE, Fish EN, Platanias LC. Type I interferon (IFN)-regulated activation of canonical and non-canonical signalling pathways. *Front Immunol*. 2020;11:606456.
- Lukhele S, Boukhaled GM, Brooks DG. Type I interferon signalling, regulation and gene stimulation in chronic virus infection. *Semin Immunol*. 2019;43:101277.
- Vannucchi AM, Lasho TL, Guglielmelli P, Biamonte F, Pardanani A, Pereira A, et al. Mutations and prognosis in primary myelofibrosis. *Leukemia*. 2013;27:1861–9.
- Roulois D, Loo Yau H, Singhania R, Wang Y, Danesh A, Shen SY, et al. DNA-demethylating agents target colorectal cancer cells by inducing viral mimicry by endogenous transcripts. *Cell*. 2015;162:961–73.
- Eppert K, Takenaka K, Lechman ER, Waldron L, Nilsson B, van Galen P, et al. Stem cell gene expression programs influence clinical outcome in human leukemia. *Nat Med*. 2011;17:1086–93.
- McCall MN, Bolstad BM, Irizarry RA. Frozen robust multiarray analysis (fRMA). *Biostatistics*. 2010;11:242–53.
- Mullally A, Bruedigam C, Poveromo L, Heidel FH, Purdon A, Vu T, et al. Depletion of Jak2V617F myeloproliferative neoplasm-propagating stem cells by interferon-alpha in a murine model of polycythemia vera. *Blood*. 2013;121:3692–702.
- Mullally A, Lane SW, Ball B, Megerdichian C, Okabe R, al-Shahrour F, et al. Physiological Jak2V617F expression causes a lethal myeloproliferative neoplasm with differential effects on hematopoietic stem and progenitor cells. *Cancer Cell*. 2010;17:584–96.
- Newman AM, Liu CL, Green MR, Gentles AJ, Feng W, Xu Y, et al. Robust enumeration of cell subsets from tissue expression profiles. *Nat Methods*. 2015;12:453–7.
- Lapidot T, Sirard C, Vormoor J, Murdoch B, Hoang T, Caceres-Cortes J, et al. A cell initiating human acute myeloid leukaemia after transplantation into SCID mice. *Nature*. 1994;367:645–8.
- Bonnet D, Dick JE. Human acute myeloid leukemia is organized as a hierarchy that originates from a primitive hematopoietic cell. *Nat Med*. 1997;3:730–7.
- Mehdipour P, Marhon SA, Ettayebi I, Chakravarthy A, Hosseini A, Wang Y, et al. Epigenetic therapy induces transcription of inverted SINES and ADAR1 dependency. *Nature*. 2020;588:169–73.
- Barbalat R, Ewald SE, Mouchess ML, Barton GM. Nucleic acid recognition by the innate immune system. *Annu Rev Immunol*. 2011;29:185–214.
- Vainchenker W, Kralovics R. Genetic basis and molecular pathophysiology of classical myeloproliferative neoplasms. *Blood*. 2017;129:667–79.
- Tefferi A, Guglielmelli P, Larson DR, Finke C, Wassie EA, Pieri L, et al. Long-term survival and blast transformation in molecularly annotated essential thrombocythemia, polycythemia vera, and myelofibrosis. *Blood*. 2014;124:2507–13; quiz 2615.
- Tefferi A, Vannucchi AM. Genetic risk assessment in myeloproliferative neoplasms. *Mayo Clin Proc*. 2017;92:1283–90.
- Yogarajah M, Tefferi A. Leukemic transformation in myeloproliferative neoplasms: a literature review on risk, characteristics, and outcome. *Mayo Clin Proc*. 2017;92:1118–28.
- Fisher DAC, Fowles JS, Zhou A, Oh ST. Inflammatory pathophysiology as a contributor to myeloproliferative neoplasms. *Front Immunol*. 2021;12:683401.
- Cominal JG, Cacemiro MC, Berzoti-Coelho MG, Pereira IEG, Frantz FG, Souto EX, et al. Bone marrow soluble mediator signatures of patients with Philadelphia chromosome-negative myeloproliferative neoplasms. *Front Oncol*. 2021;11:665037.
- Hasselbalch HC, Silver RT. New perspectives of interferon-alpha2 and inflammation in treating Philadelphia-negative chronic myeloproliferative neoplasms. *Hema*. 2021;5:e645.
- Lussana F, Rambaldi A. Inflammation and myeloproliferative neoplasms. *J Autoimmun*. 2017;85:58–63.
- Hasselbalch HC. Perspectives on chronic inflammation in essential thrombocythemia, polycythemia vera, and myelofibrosis: is chronic inflammation a trigger and driver of clonal evolution and development of accelerated atherosclerosis and second cancer? *Blood*. 2012;119:3219–25.
- Fleischman AG, Aichberger KJ, Luty SB, Bumm TG, Petersen CL, Doratotaj S, et al. TNF-alpha facilitates clonal expansion of

- JAK2V617F positive cells in myeloproliferative neoplasms. *Blood*. 2011;118:6392–8.
30. Huangfu WC, Qian J, Liu C, Liu J, Lokshin AE, Baker DP, et al. Inflammatory signalling compromises cell responses to interferon alpha. *Oncogene*. 2012;31:161–72.
  31. Katlinski KV, Gui J, Katlinskaya YV, Ortiz A, Chakraborty R, Bhattacharya S, et al. Inactivation of interferon receptor promotes the establishment of immune privileged tumour microenvironment. *Cancer Cell*. 2017;31:194–207.
  32. Araya RE, Goldszmid RS. IFNAR1 degradation: a new mechanism for tumour immune evasion? *Cancer Cell*. 2017;31:161–3.
  33. Costa AFO, Olops Marani L, Mantello Bianco T, Queiroz Arantes A, Aparecida Lopes I, Antonio Pereira-Martins D, et al. Altered distribution and function of NK-cell subsets lead to impaired tumour surveillance in JAK2V617F myeloproliferative neoplasms. *Front Immunol*. 2022;13:768592.
  34. Colombo AR, Zubair A, Thiagarajan D, Nuzhdin S, Triche TJ, Ramsingh G. Suppression of transposable elements in leukemic stem cells. *Sci Rep*. 2017;7:7029.
  35. Hasselbalch HC, Holmstrom MO. Perspectives on interferon-alpha in the treatment of polycythemia vera and related myeloproliferative neoplasms: minimal residual disease and cure? *Semin Immunopathol*. 2019;41:5–19.
  36. How J, Hobbs G. Use of interferon alfa in the treatment of myeloproliferative neoplasms: perspectives and review of the literature. *Cancers (Basel)*. 2020;12:1954.
  37. Mosca M, Hermange G, Tisserand A, Noble R, Marzac C, Marty C, et al. Inferring the dynamics of mutated hematopoietic stem and progenitor cells induced by IFNalpha in myeloproliferative neoplasms. *Blood*. 2021;138:2231–43.
  38. Kiladjian JJ, Giraudier S, Cassinat B. Interferon-alpha for the therapy of myeloproliferative neoplasms: targeting the malignant clone. *Leukemia*. 2016;30:776–81.
  39. Kjaer L, Cordua S, Holmström MO, Thomassen M, Kruse TA, Pallisgaard N, et al. Differential dynamics of CALR mutant allele burden in myeloproliferative neoplasms during interferon alfa treatment. *PLoS One*. 2016;11:e0165336.
  40. Masarova L, Patel KP, Newberry KJ, Cortes J, Borthakur G, Konopleva M, et al. Pegylated interferon alfa-2a in patients with essential thrombocythaemia or polycythaemia vera: a post-hoc, median 83 month follow-up of an open-label, phase 2 trial. *Lancet Haematol*. 2017;4:e165–75.
  41. Iantotto JC, Chauveau A, Boyer-Perrard F, Gyan E, Laribi K, Cony-Makhoul P, et al. Benefits and pitfalls of pegylated interferon-alpha2a therapy in patients with myeloproliferative neoplasm-associated myelofibrosis: a French Intergroup of Myeloproliferative neoplasms (FIM) study. *Haematologica*. 2018;103:438–46.
  42. Cassinat B, Verger E, Kiladjian JJ. Interferon alfa therapy in CALR-mutated essential thrombocythemia. *N Engl J Med*. 2014;371:188–9.
  43. Marti-Carvajal AJ, Anand V, Sola I. Janus kinase-1 and Janus kinase-2 inhibitors for treating myelofibrosis. *Cochrane Database Syst Rev*. 2015;CD010298.
  44. Cervantes F, Pereira A. Does ruxolitinib prolong the survival of patients with myelofibrosis? *Blood*. 2017;129:832–7.
  45. Griesshammer M, Saydam G, Palandri F, Benevolo G, Egyed M, Callum J, et al. Ruxolitinib for the treatment of inadequately controlled polycythemia vera without splenomegaly: 80-week follow-up from the RESPONSE-2 trial. *Ann Hematol*. 2018;97:1591–600.
  46. Austin RJ, Straube J, Bruedigam C, Pali G, Jacquelin S, Vu T, et al. Distinct effects of ruxolitinib and interferon-alpha on murine JAK2V617F myeloproliferative neoplasm hematopoietic stem cell populations. *Leukemia*. 2020;34:1075–89.
  47. Sorensen AL, Mikkelsen SU, Knudsen TA, Bjørn ME, Andersen CL, Bjerrum OW, et al. Ruxolitinib and interferon-alpha2 combination therapy for patients with polycythemia vera or myelofibrosis: a phase II study. *Haematologica*. 2020;105:2262–72.
  48. Mikkelsen SU, Kjaer L, Bjørn ME, Knudsen TA, Sørensen AL, Andersen CBL, et al. Safety and efficacy of combination therapy of interferon-alpha2 and ruxolitinib in polycythemia vera and myelofibrosis. *Cancer Med*. 2018;7:3571–81.
  49. Chiappinelli KB, Strissel PL, Desrichard A, Li H, Henke C, Akman B, et al. Inhibiting DNA methylation causes an interferon response in cancer via dsRNA including endogenous retroviruses. *Cell*. 2015;162:974–86.
  50. Danilov AV, Relias V, Feeney DM, Miller KB. Decitabine is an effective treatment of idiopathic myelofibrosis. *Br J Haematol*. 2009;145:131–2.
  51. Badar T, Kantarjian HM, Ravandi F, Jabbour E, Borthakur G, Cortes JE, et al. Therapeutic benefit of decitabine, a hypomethylating agent, in patients with high-risk primary myelofibrosis and myeloproliferative neoplasm in accelerated or blastic/acute myeloid leukemia phase. *Leuk Res*. 2015;39:950–6.
  52. Jones PA, Ohtani H, Chakravarthy A, De Carvalho DD. Epigenetic therapy in immune-oncology. *Nat Rev Cancer*. 2019;19:151–61.
  53. Thepot S, Itzykson R, Seegers V, Raffoux E, Quesnel B, Chait Y, et al. Treatment of progression of Philadelphia-negative myeloproliferative neoplasms to myelodysplastic syndrome or acute myeloid leukemia by azacitidine: a report on 54 cases on the behalf of the Groupe Francophone des Myelodysplasies (GFM). *Blood*. 2010;116:3735–42.
  54. Jabbour E, Short NJ, Montalban-Bravo G, Huang X, Bueso-Ramos C, Qiao W, et al. Randomized phase 2 study of low-dose decitabine vs low-dose azacitidine in lower-risk MDS and MDS/MPN. *Blood*. 2017;130:1514–22.
  55. Stomper J, Rotondo JC, Greve G, Lubbert M. Hypomethylating agents (HMA) for the treatment of acute myeloid leukemia and myelodysplastic syndromes: mechanisms of resistance and novel HMA-based therapies. *Leukemia*. 2021;35:1873–89.
  56. Lock M, Luque Paz D, Hansen N, Almeida Fonseca T, Usart MARC, Rai S, et al. Combination of 5-azacytidine and Pegifna is able to overcome resistance in JAK2-V617F positive MPN with loss of *Dnmt3a*. *Blood*. 2022;140(Suppl. 1):3876–7.

## SUPPORTING INFORMATION

Additional supporting information can be found online in the Supporting Information section at the end of this article.

**How to cite this article:** de Castro FA, Mehdipour P, Chakravarthy A, Ettayebi I, Loo Yau H, Medina TS, et al. Ratio of stemness to interferon signalling as a biomarker and therapeutic target of myeloproliferative neoplasm progression to acute myeloid leukaemia. *Br J Haematol*. 2024;204(1): 206–220. <https://doi.org/10.1111/bjh.19107>